



PERGAMON

Available online at [www.sciencedirect.com](http://www.sciencedirect.com)

SCIENCE @ DIRECT®

Scripta Materialia 48 (2003) 1337–1342



[www.actamat-journals.com](http://www.actamat-journals.com)

# Fabrication of functionally graded TiC/Ti composites by Laser Engineered Net Shaping

Weiping Liu<sup>\*</sup>, J.N. DuPont

*Department of Materials Science and Engineering, Lehigh University, 5 E. Packer Avenue, Bethlehem, PA 18015, USA*

Received 3 December 2002; received in revised form 7 January 2003; accepted 13 January 2003

---

## Abstract

Crack-free functionally graded TiC/Ti composite materials were fabricated by laser engineered net shaping (LENS), with compositions changing from pure Ti to approximately 95 vol% TiC. By delivering the constituent materials from different powder feeders and through process control, the LENS process can be used for the fabrication of functionally graded materials.

© 2003 Acta Materialia Inc. Published by Elsevier Science Ltd. All rights reserved.

*Keywords:* LENS processing; FGM; Composites; Microstructure; TiC carbide

---

## 1. Introduction

Functionally graded materials (FGMs) are a class of advanced materials of which the composition and microstructure change gradually from one side to the other, resulting in a corresponding variation in the properties. The concept of FGMs was first proposed in 1987 to develop heat-resistant materials for the propulsion system and airframe of space planes [1]. Since then, much research has been done to develop FGMs for various applications by using gradients in physical, chemical, biochemical, and mechanical properties [2–4]. The main characteristic that distinguishes FGMs from conventional composite materials is the tailoring of graded composition and micro-

structure in an intentional manner according to the distribution of properties needed to achieve the desired function [2]. Therefore, FGMs can be utilized for the realization of innovative properties and functions to meet performance requirements that vary with location within a component. Among various FGMs, ceramic/metal FGMs are of great practical interest. These FGMs accomplish the integration of normally incompatible functions such as the refractoriness and wear resistance of ceramics and the toughness of metals for structural applications. The gradual compositional variations from ceramics at one surface to metals at the other lead to unique advantages of smooth transition in thermal stresses along the thickness direction and minimized stress concentration at the interface.

There are several methods such as CVD/PVD, plasma spraying, powder metallurgy and self-propagating high-temperature synthesis (SHS), which are currently used for producing FGMs.

---

<sup>\*</sup> Corresponding author. Tel.: +1-6107584270; fax: +1-6107586407.

E-mail address: [wel2@lehigh.edu](mailto:wel2@lehigh.edu) (W. Liu).

CVD/PVD and plasma spraying are generally applied for fabrication of functionally graded coatings [3], and the FGM coatings made by plasma spraying are not dense. Although powder metallurgy and SHS processes can be utilized for producing bulk FGMs, the shapes and sizes are usually limited because of the use of dies for pressure-aided densification. Laser engineered net shaping (LENS) is a solid freeform fabrication process, which involves laser processing fine powders into fully dense three-dimensional shapes directly from a computer-aided design model. The LENS process is able to fabricate complex prototypes in near-net shape, leading to time and machining cost savings. A variety of metals and alloys have been deposited by the LENS process, such as H13 steel, 316 stainless steel, nickel-base superalloys and titanium alloys [5–8]. This process also exhibits potential for fabrication of FGMs and structures [5]. In this work, a TiC/Ti ceramic/metal FGM was fabricated by LENS processing. The microstructure of the FGM was characterized and the hardness distribution was also evaluated.

## 2. Experimental procedures

The materials used in this work were TiC powder (99.9% purity) from Atlantic Equipment Engineers and Ar gas-atomized CP Ti powder (>99.6% purity) obtained from PyroGenesis company. All the powders have a mesh size of  $-100/+325$  (particle sizes between 45 and 150  $\mu\text{m}$ ). A hot-rolled Ti–6Al–4V plate of 3.175 mm thickness was used as the substrate material, which had a composition of 6.1 Al, 4.3 V (in wt.%). The substrate was ground with 320 grit SiC paper, and then degreased using acetone and ethanol before deposition.

An Optomec LENS™ 750 system was used in this study. The LENS system consists of a Nd:YAG laser, a four-nozzle coaxial powder feed system, a controlled environment glove box and a motion control system. The Nd:YAG laser has a 0.5–1 mm-diameter circular beam at the focal zone with the Gaussian intensity distribution and a maximum output power of 750 W. The LENS system is equipped with a melt pool sensor (MPS) subsystem to provide closed-loop control. The MPS subsystem

is designed to automatically adjust the power of the laser to maintain a constant surface area of the molten pool, which is useful for deposition of variable materials (e.g. FGM deposits) and eliminating melt pool size variations that can occur due to geometrical changes in the part. The powder delivering nozzles in the LENS system are arranged so that the powder streams converge at the focal point of the laser beam. Two powder feeders were used to deliver Ti and TiC powders separately. The powders were mixed in situ during feeding from the powder feeders to the nozzles, and their feed rates were controlled individually by regulating the rotational speed of each powder feeder. For fabrication of the FGM, the rotational speed for the powder feeder of one material varied from zero to a maximum which was set according to the laser power and traverse speed used. The rotational speed for the other powder feeder carrying the second material varied from a maximum to zero stepwise as the number of layers increased. The variation of rotational speed for the powder feeding was program controlled, with a minimal step of 0.1 rotations per minute used in the experiment. The FGM samples had a size of 12.7 mm  $\times$  12.7 mm  $\times$  20 layers. For comparison, homogeneous TiC and TiC/Ti composite (with fixed TiC vol%) deposits were also produced. A 420 W laser power and an 8.5 mm/s traverse speed were used in this work. Successive layers were deposited with the bead lines of two adjacent layers at an angle of 90°. The layer thickness, hatch spacing, and stand-off distance were set at 0.38, 0.38 and 152.4 mm respectively. The oxygen level in the glove box was kept below 6 ppm during processing. Light optical microscopy (LOM), scanning electron microscopy (SEM) coupled with X-ray energy dispersive spectrum (EDS) analysis, and X-ray diffraction (XRD) were used for microstructure and phase analysis. Microhardness measurements were conducted using a Vickers indenter under a 300 g load.

## 3. Results and discussion

Fig. 1 shows the results of XRD analyses conducted on the horizontal surfaces of the bottom and top layers and on the vertical cross-section of

the FGM deposit, respectively. The results indicate that the LENS FGM deposit contains  $\alpha$ -Ti (hcp) and TiC (B1 NaCl type). The bottom layer consists essentially of  $\alpha$ -Ti with a very small amount of TiC while the top layer is mostly TiC with a small amount of  $\alpha$ -Ti. Fig. 2(a) shows a cross-sectional LOM photomicrograph of the FGM deposit. A crack-free and dense TiC/Ti functionally graded composite was fabricated. Fig. 2(b)–(g) show SEM photomicrographs of the microstructures with increasing TiC contents in different locations of the FGM deposit. EDS analysis of the unmelted TiC particles, the matrix and dendritic phases indicated that carbon peaks appear in the unmelted TiC and the dendritic phase. These results confirm that the dendritic phase is resolidified primary TiC. In addition to the dendritic shape, a small amount of much finer equiaxed TiC particles can also be observed in the microstructure (Fig. 2(b)). The unmelted TiC particles are in a large blocky shape (Fig. 2(e)). It can be seen from Fig. 2 that the microstructure of the LENS FGM gradually changes from pure Ti to approximately 95 vol% TiC with the variation in composition.

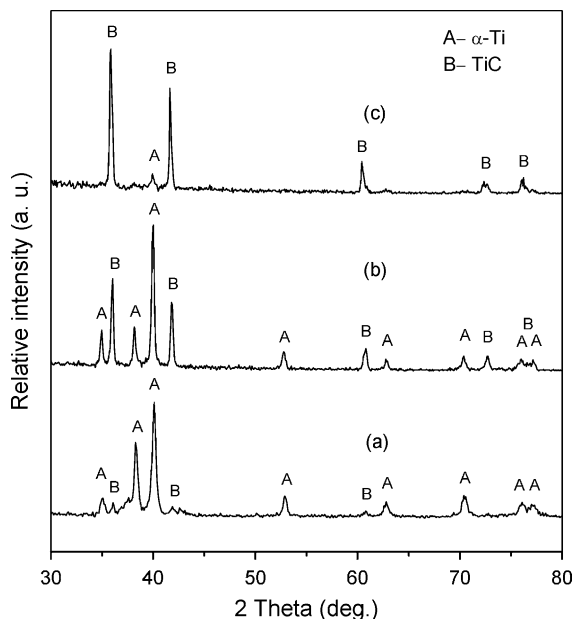


Fig. 1. XRD patterns obtained from the different locations in the FGM deposit: (a) first layer; (b) cross-section; and (c) last layer.

The laser absorption coefficient ( $\alpha$ ) of a material is a function of temperature, its electrical resistivity and the laser's wavelength [9]. The larger the electrical resistivity of a material, the higher its laser absorption coefficient. The values of electrical resistivity for TiC and Ti at room temperature are 138–188  $\mu\Omega\text{cm}$  [10] and 42–55  $\mu\Omega\text{cm}$  [11], respectively. Therefore, the TiC powder particles have a higher laser absorption coefficient. In addition, the heat conductivity of TiC is lower. As a result, partial melting of the TiC powder, in spite of its high melting point, would occur at the periphery of the particles. Moreover, dissolution of TiC particles into the molten Ti is also expected during LENS processing. Consequently, the melted/dissolved TiC would resolidify during the cooling process. The different morphologies of the resolidified TiC phase can be interpreted according to the solidification process. At lower TiC contents in the FGM deposit, very few large, blocky unmelted TiC particles were observed. This indicates that most of the injected TiC particles were melted/dissolved (Fig. 2(b)–(d)). According to the binary Ti–C phase diagram [12], C concentrations from approximately 0.5 to 16 wt.% C will form primary TiC during solidification. When the temperature decreased to the eutectic temperature (1648 °C), TiC formed in equiaxed shape in the eutectic (consisting of TiC and  $\beta$ -Ti). As the content of TiC in the injected powder mixture increased, the amount of unmelted/undissolved TiC increased in the melted pool. The resultant microstructure consists of resolidified TiC/Ti distributed in the network of unmelted TiC (Fig. 2(e) and (f)). Finally, when the content of Ti in the injected powder mixture decreased to a minimum ( $\sim 5$  vol%), the unmelted TiC particles appear to be bonded to each other by the resolidified TiC particles, with the minimum Ti phase distributed in the interparticle boundaries (Fig. 2(g)).

It is known that TiC has an fcc lattice structure in which the C atoms reside inside the octahedral interstices. According to the Ti–C phase diagram [12], TiC has an extraordinarily wide range of composition (from approximately 32 to 49 at.% C) depending on the degree of carbon vacancies. From the XRD data of a Ti–10vol%TiC composite deposit free of unmelted TiC particles, the

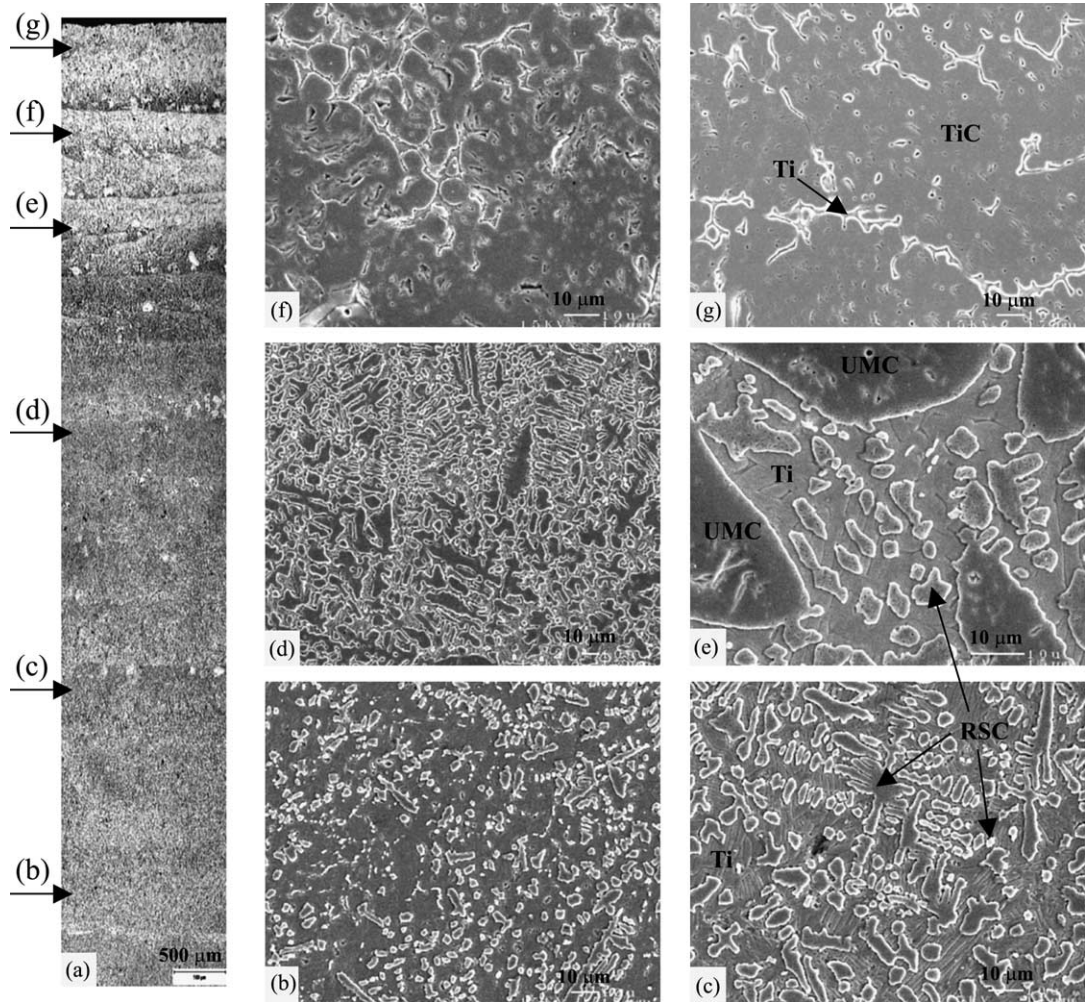


Fig. 2. Microstructures of the FGM deposit: (a) LOM photomicrograph of the deposit; (b)–(g) SEM photomicrographs with increasing TiC contents in different locations (UMC and RSC denote unmelted and resolidified TiC carbide respectively).

lattice parameter of the resolidified TiC is measured to be 4.2975 Å from the TiC (3 1 1) diffractive peak. The stoichiometric TiC has a lattice parameter of 4.3278 Å [13]. The lattice parameters for  $\text{TiC}_{0.75}$  and  $\text{TiC}_{0.55}$  have been determined to be 4.3122 and 4.2832 Å respectively [14]. Therefore, the resolidified TiC in the LENS deposit is non-stoichiometric, with its composition estimated to be  $\text{TiC}_{0.65}$  through interpolation by assuming a linear relationship in the composition range between  $\text{TiC}_{0.75}$  and  $\text{TiC}_{0.55}$ .

It is interesting to note that crack-free FGM deposits with TiC contents up to 95 vol% were

fabricated by the LENS process. By comparison, an attempt to directly deposit eight layers of 100% TiC onto the Ti–6Al–4V substrate resulted in large vertical cracks throughout the deposit and small transverse cracks near the substrate (Fig. 3(a)). In another homogeneous Ti–80vol%TiC composite deposit, a long transverse crack was observed near the deposit/substrate interface (Fig. 3(b)). The crack was found to originate near the interface as shown schematically in Fig. 3(c). It is believed that these cracks resulted from a high level of combined processing-generated thermal stresses and interfacial mismatch stresses. In brittle materials, relief of

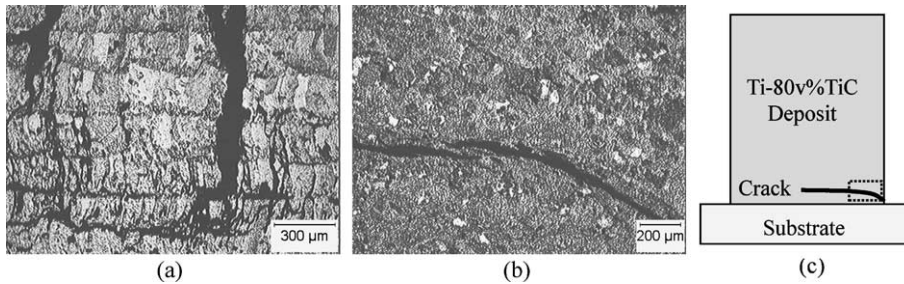


Fig. 3. Cracks observed in the homogeneous deposits: (a) full TiC deposit; (b) Ti-80vol%TiC composite deposit; (c) a schematic showing the originating position of the crack in the composite deposit.

thermal stresses can generally only occur in the form of cracking, whereas in ductile materials the stress relief can be accomplished by plastic deformation. In the FGM deposit, both kinds of stresses can be significantly reduced and the ductility can be improved by the gradual compositional variations, and cracking can therefore be avoided.

Fig. 4 shows the Vickers microhardness distribution of the FGM deposit along the thickness direction. The hardness in the deposit increases from about 200 Vickers hardness number (VHN) at the Ti side to approximately 2300 VHN at the top layer as the TiC content increases. The non-linear variation of hardness might be due to the fact that the resolidified non-stoichiometric  $TiC_x$  has a lower hardness value than the unmelted TiC. In spite of the non-linear distribution, the hardness exhibits a gradual and continuous variation in the FGM. The distribution of hardness and other

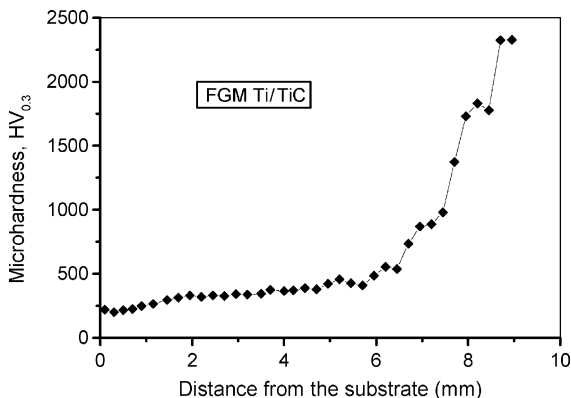


Fig. 4. Hardness distribution of the LENS fabricated Ti/TiC functionally graded composite.

properties can also be tailored by the design of compositional profiles via controlling the feed rates of the constituent materials and dilutions between the layers. Future study in these aspects is needed.

#### 4. Conclusions

A functionally graded TiC/Ti composite material was successfully fabricated by LENS processing, with the composition changing from pure Ti to approximately 95 vol% TiC. In comparison to homogeneous composite deposits of high TiC contents, the FGM fabrication effectively prevents the formation of cracks. With the ease of delivering the constituent materials and available process control, the LENS process can be used for the fabrication of FGMs.

#### Acknowledgements

The authors gratefully acknowledge support of this work by the National Science Foundation through a PECASE Award, grant no. DMI 9983968, made through the Division of Manufacturing and Industrial Innovation of NSF.

#### References

- [1] Niino M, Hirai T, Watanabe R. J Jpn Soc Comp Mater 1987;13:257–64.
- [2] Kawasaki A, Watanabe R. Ceram Int 1997;23:73–83.

- [3] Prchlik L, Sampath S, Gutleber J, Bancke G, Ruff AW. *Wear* 2001;249:1103–15.
- [4] Pei YT, Ocelik V, De Hosson JThM. *Acta Mater* 2002;50:2035–51.
- [5] Griffith ML, Harwell LD, Romero JT, Schlienger E, Atwood CL, Smugeresky JE. Proc 8th Solid Freeform Fabrication Symp 1997. University of Texas Austin, p. 387–92.
- [6] Lewis GK, Schlienger E. *Mater Design* 2000;21:417–23.
- [7] Kobryn PA, Moore EH, Semiatin SL. *Scripta Mater* 2000;43:299–305.
- [8] Schwendner KI, Banerjee R, Collins PC, Brice CA, Fraser HL. *Scripta Mater* 2001;45:1123–9.
- [9] Duley WW. *CO<sub>2</sub> lasers: effects and applications*. NY: Academic Press; 1976. p. 136.
- [10] Toth LE. *Transition metal carbides and nitrides*. NY: Academic Press; 1971. p. 187.
- [11] Boyer R, Welsch G, Collings EW. *Materials properties handbook: titanium alloys*. Materials Park, OH: ASM International; 1994. 125.
- [12] *ASM Handbook Vol 3 Alloy Phase Diagrams* 1992. ASM Intl: Materials Park, OH: p. 2–114.
- [13] JCPDS, International Center for Diffraction Data. *Powder Diffraction File, PCPDFWIN v. 2.1 (No. 73–0472)* 2001.
- [14] Capaldi MJ, Wood JV. *J Mater Synth Proc* 1996;4:245–53.